



International Commission on Illumination  
Commission Internationale de l'Eclairage  
Internationale Beleuchtungskommission

# THE PHANTOM ARRAY EFFECT EXPLAINED USING SIMPLE FORMULAS

Martinsons, C., et al.

DOI 10.25039/x051.2025/g3akta

This article is also published as part of:

Proceedings of the CIE 2025 Midterm Meeting Vienna, Austria, July 4-11, 2025:  
Scientific Conference (July 7-9, 2025)

DOI 10.25039/x051.2025

in

Proceedings of the CIE (International Commission on Illumination)

ISSN no. 3061-015X (print), 3061-0168 (online)

The paper has undergone double-blind peer review and its final version has been presented at the CIE 2025 Midterm Meeting, Vienna, Austria, July 4–11, 2025.

© CIE 2025

All rights reserved. This work is licensed under the Creative Commons Attribution-NonCommercial 4.0 International License (<https://creativecommons.org/licenses/by-nc/4.0/>). Any mention of organizations or products does not imply endorsement by the CIE.

CIE Central Bureau  
Babenbergerstrasse 9/9A  
A-1010 Vienna, Austria  
Tel.: +43 1 714 31 87  
e-mail: [ciecb@cie.co.at](mailto:ciecb@cie.co.at) — [www.cie.co.at](http://www.cie.co.at)

# THE PHANTOM ARRAY EFFECT EXPLAINED USING SIMPLE FORMULAS

Martinsons C.<sup>1</sup>, Kong, X.<sup>2</sup>, Heynderickx I.<sup>2</sup>, Tengelin M.N.<sup>3</sup>, Kallberg S.<sup>3</sup>

<sup>1</sup> Centre Scientifique et Technique du Bâtiment, Saint Martin d'Hères, France, <sup>2</sup> Eindhoven University of Technology, Eindhoven, The Netherlands, <sup>3</sup> RISE Research Institutes of Sweden, Borås, Sweden

christophe.martinsons@cstb.fr

## Abstract

The phantom array effect is a visual effect perceived by a human observer when making rapid eye movements across a light source exhibiting temporal light modulation at frequencies between about one hundred Hz and a few kHz: a series of multiple spurious images of the light source is seen in the direction of the eye saccade. This phenomenon may create discomfort when accomplishing visual tasks involving eye movements, such as driving or walking. In this paper, we provide a simple description of the phantom array effect by deriving formulas predicting its spatial and temporal features perceived in the field of view. This approach provides a framework to study how the visibility of the phantom array effect is influenced by the shape of the source, its luminance, the surrounding and background luminance, the modulation frequency and waveform, and the individual visual acuity.

*Keywords:* Temporal Light Modulation, Phantom Array Effect, Modelling, Visibility, Contrast Sensitivity Function, Eye Tracking, Saccade, Light Source

## 1 Introduction

The phantom array effect (PAE) is a visual effect that can be perceived when a light source exhibits temporal light modulation (TLM) (CIE, 2022) and when the eyes move rapidly across the field of view. Unlike direct flicker and stroboscopic effects, the PAE occurs at rather high modulation frequencies, typically from 100 Hz up to several kHz. This frequency range is unfortunately the most widely used by dimming systems based on pulse-width modulation. This may explain why the PAE is visible with some lighting systems used in dimmed conditions.

The phantom array is a series of multiple spurious images of the light source formed in the visual field along the direction of the eye saccade. For most people, the PAE is a source of visual discomfort and distraction. Sensitive people may experience severe forms of light aversion (Martinsons et al., 2024; Miller, 2024) from the phantom array effect.

Recent research initiatives have led to a better understanding of the occurrence of the PAE (Brown et al., 2020; Kang et al., 2022; Kong et al., 2023; Lee et al., 2018; Miller et al., 2023). Several sensitivity curves expressing visibility as a function of modulation frequency were measured and a visibility metric called PAVM (Phantom Array Visibility Measure) has been proposed by one research team (Tan et al., 2024). However, the basic characteristics of the perceived visual pattern have not been clearly explained. We provide here a description of the phantom array effect based on simple equations predicting its spatial and temporal features, as perceived in the visual field. A general framework based on the linear theory of the human visual system is given to study the parameters influencing the visibility of the PAE.

## 2 The formation of the phantom array effect

When the eyes scan a scene from left to right across a temporally modulated light source, the phantom array is seen as a pattern of multiple images of the source, only visible during the saccade. The phenomenon has been described in (Hershberger and Jordan, 1998). This pattern appears to be entirely localized on the right side of the light source in its final position. Although it might be hard to notice, the phantom images are produced one after another in a sequential

order, following the reverse direction of the saccade. Each successive phantom image is seen closer and closer to the final position of the light source itself (Figure 1). The photograph in Figure 1b was taken while rapidly moving the camera from left to right. The resulting effect is not exactly what would be perceived during an eye saccade. A phenomenon called saccadic suppression (Matin, 1975) momentarily reduces the perception of the blur caused by the retinal motion during a saccade. Remarkably, the phantom array is not suppressed and remains visible during the saccade.

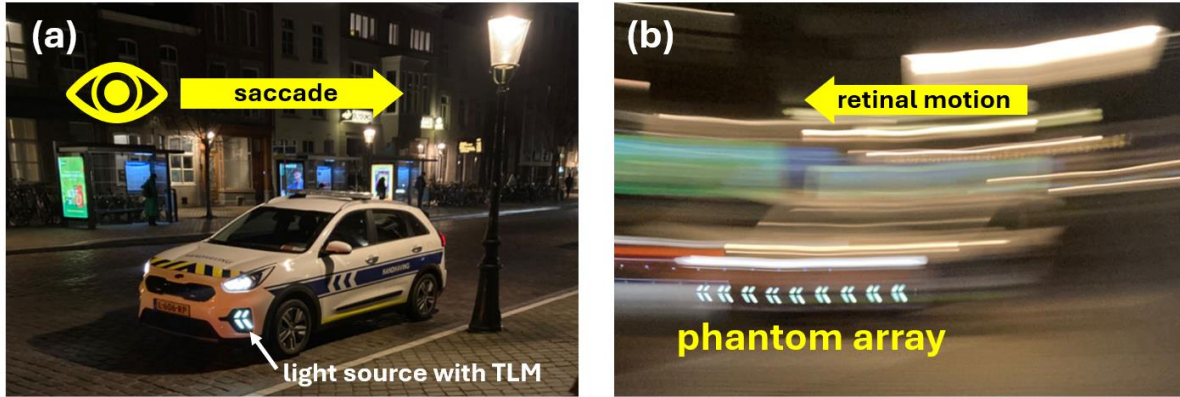


**Figure 1 – Formation of the phantom array (a). The eyes make a saccade from the left to the right. (b) The phantom array effect appears during the retinal motion resulting from the saccade.**

**2.1 The geometric features of the phantom array**

The pattern of multiple light source images can be considered as a periodic pattern, like a grating, appearing in the field of view during the saccade (Figure 1). Each individual image is formed during a cycle of the temporal light waveform. Table 1 gives the list of parameters that are needed to characterize the spatial features of the phantom array.

**Table 1 – Parameters used to characterize the spatial features of the phantom array**

	Parameter	Symbol
<b>Light source</b>	Modulation frequency	$f$ (Hz)
	Angular size of source	$l$ (deg)
<b>Observer</b>	Saccade amplitude	$A$ (deg)
	Saccade speed	$\omega$ (deg·s <sup>-1</sup> )

The pattern is defined by the number of images  $N$  and their angular period  $\delta$  that can be calculated using Equations (1) and (2):

$$N = \frac{Af}{\omega} \tag{1}$$

$$\delta = \frac{\omega}{f} \tag{2}$$

When the angular period of the phantom array is smaller than the angular size of the light source ( $l$ ), the multiple images overlap, making the PAE invisible. Therefore, there is a relationship between the size of source and the highest modulation frequency for the PAE. This frequency, noted  $f_{high}$ , can be defined using Equation (3):

$$f_{high} = \frac{\omega}{l} \tag{3}$$

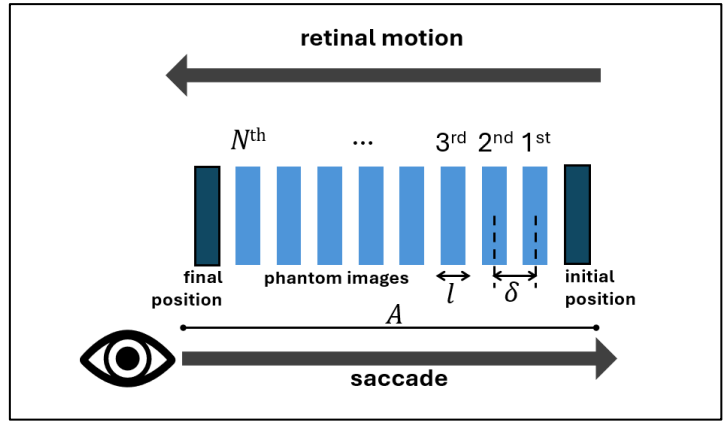


**Figure 2 – Illustration of the number of images and angular period of the phantom array**

For instance, if an observer makes a saccade with a typical speed of  $300 \text{ deg}\cdot\text{s}^{-1}$ , the PAE cannot be perceived for a thin light source extending over a  $0,1^\circ$  angle if the modulation frequency is higher than 3 000 Hz, even with a modulation depth of 100%.

Equations (1) and (2) also show that if the modulation frequency is too low, there are not enough phantom images to form an array. At least one phantom image should be visible between the initial and final positions of the retinal image of the light source (Figure 3). This case corresponds to a saccade lasting exactly two modulation cycles. Therefore, the lowest angular period is half the saccade amplitude. Introducing this value in Equation (2), the low frequency geometric limit can be expressed by Equation (4):

$$f_{low} = \frac{2\omega}{A} \tag{4}$$

The oculo-motor muscles of the eyes allow us to perform effortless saccades up to an amplitude of about  $20^\circ$  (Bahill et al., 1975). The peak saccade speed corresponding to this amplitude is about  $500 \text{ deg}\cdot\text{s}^{-1}$  (Bahill et al., 1975). In this case, Equation (4) yields a low frequency geometric limit of about 50 Hz.

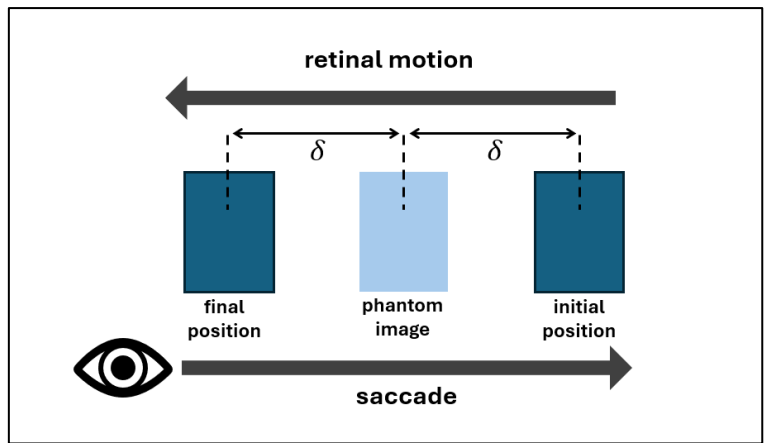


**Figure 3 – Low frequency geometric limit of the phantom array effect**

**2.2 The temporal features of the phantom array**

The pattern formed by the phantom images is transient. All the images are formed during the duration  $t$  of the saccade according to Equation (5):

$$t = \frac{A}{\omega} \tag{5}$$

The peak angular speed of the saccade and its duration both increase with its amplitude (Bahill et al., 1975). Under typical viewing conditions, voluntary saccades with amplitudes ranging from 1° to 20° exhibit peak angular velocities of 50-500 deg·s<sup>-1</sup>, with corresponding durations of 20-50 ms (Bahill et al., 1975). The typical value is 40 ms (Castet, 2000). In general, the duration of larger saccades cannot exceed 100 ms (Bahill et al., 1975), a value which can be considered as the maximum duration of the phantom array effect.

During a saccade, a single phantom image is created at each modulation cycle of the light source. For a square wave with a duty cycle of 0,5, an individual image is formed on the retina during a duration  $\tau$  given by one half of the modulation period, according to the Equation (6):

$$\tau = \frac{1}{2f} \tag{6}$$

For instance, with a modulation frequency of 500 Hz, each phantom image is formed on the retina during 1 ms. The decay of the phantom array is linked to the persistence of each phantom image. This aspect was addressed in (Kang and Lee, 2023) by considering Ricco's law to include the influence of the individual area of the phantom images on their excitation and relaxation times. Riccos' law works well for images of very small area (less than the size of the receptive field) and low luminance. However, these conditions do not always apply to the phantom array.

### 3 A general framework to predict the visibility of the phantom array effect

A general modelling framework predicting the visibility of the phantom array is described below. By applying the linear theory of the human visual system introduced by De Lange (De Lange, 1952) and generalized by Campbell and Robson (Campbell 1968), it is possible to study the visibility of the phantom array as a function of its spatial frequency  $k$ , defined as the inverse of the angular period. It can be expressed in cycle per degree (cpd) using Equation (7):

$$k = \frac{1}{\delta} = \frac{f}{\omega} \tag{7}$$

When the temporal waveform of the light source is not a pure sine wave, it includes multiple modulation frequencies such as higher-order harmonics. Each harmonic induces its own spatial frequency which is determined using Equation (7). The lowest relevant spatial frequency corresponds to the low frequency geometric limit of Equation (4). With a saccade amplitude of 20°, the lowest spatial frequency of the phantom array is 0,1 cpd (i.e., = 50 Hz / 500 deg·s<sup>-1</sup>). Considering the effect of the size of the light source, the highest relevant spatial frequency corresponds to the high frequency geometric limit (determined by overlapping phantom images) given by Equation (3). For a light source with an angular extent of 0,1°, the highest spatial frequency is 10 (i.e., = 1 / 0,1) cpd. If the light source is infinitely thin, then the highest spatial frequency of the phantom array would depend on the visual acuity of the observer as explained below.

A general equation expressing the visibility of the phantom array in the spatial frequency domain should incorporate two terms: a quantity describing the stimulus and another quantity describing the visual response. The stimulus is the contrast of the phantom array formed on the retina. For any given value of the spatial frequency  $k$ , the stimulus  $C(k)$  can be calculated as the product of the Fourier amplitude of the temporal light waveform normalized by the steady-state (DC) amplitude of the temporal modulation waveform, and the spatial frequency component of the light source in the direction of the saccade divided by the surround luminance of the light source, as expressed in Equation (8):

$$C(k) = \frac{\mathcal{T}(k)}{\mathcal{T}_{dc}} \cdot \frac{\mathcal{L}(k)}{\mathcal{L}_{sur}} \tag{8}$$

where

$\mathcal{T}(k)$  is the Fourier component of the temporal light waveform, scaled using Equation (7);

$\mathcal{T}_{dc}$  is the DC value of the temporal light waveform;

$\mathcal{L}(k)$  is the Fourier component of the angular distribution of the light source luminance, in the direction of the saccade;

$\mathcal{L}_{sur}$  is the luminance of the zone surrounding the light source.

Equation (8) shows that the contrast of the phantom array is determined by a temporal term (the modulation depth of the light source) and a spatial term (the contrast of the light source with its surrounding background). These two components act in a similar way on the PAE. The visibility of the phantom array can be reduced in the same proportion by reducing the modulation depth or by reducing the luminance contrast.

The visual response to the PAE is determined by the contrast sensitivity function  $CSF_{PA}(k)$  of the observer in the specific conditions of the phantom array. Combining the stimulus and response terms, the visibility  $V(k)$  of the phantom array at a given spatial frequency  $k$  can be given by Equation (9):

$$V_{PA}(k) = C(k) \cdot CSF_{PA}(k) \quad (9)$$

The overall visibility of the PAE can be determined by summing all the spatial frequency components ( $k_1, k_2 \dots, k_n$ ). Following the methodology presented in (Perz, 2015), the summation of frequency components could be defined as a Minkowski norm with an exponent  $p$ , as shown in Equation (10):

$$V_{PA} = \left( \sum_{i=1}^n [V_{PA}(k_i)]^p \right)^{\frac{1}{p}} \quad (10)$$

Using the results of an experimental study (Miller et al., 2023), the phantom array visibility metric PAVM was recently defined (Tan et al., 2024) by using a weighted sum of the Fourier components of the temporal waveform. The authors found a Minkowski exponent of 2,1, a value close to 2 corresponding to a quadratic sum of the different components.

The model defined by Equation (8), (9) and (10) includes the effects of all the factors that are currently known to influence the visibility of the PAE. Table 2 details these parameters and indicates their respective influence on the different terms of the model.

**Table 2 – Parameters influencing the visibility of the phantom array effect**

	Model quantity	Factor influencing the PAE	Detail
<b>Stimulus</b>	Fourier component of temporal waveform $\mathcal{T}(k)/\mathcal{T}_{dc}$	Modulation depth	Each frequency component is considered
		Frequency components of TLM	
	Fourier component of source luminance distribution $\mathcal{L}(k)/\mathcal{L}_{sur}$	Size of source	Each spatial frequency is considered
		Luminance of TLM light source	
Luminance of surrounding			
	Luminance contrast		
<b>Observer</b>	Spatial frequency $k$	Saccade velocity	Peak angular velocity
	Contrast sensitivity function during eye saccade $CSF_{PA}(k)$	Individual differences	Effect of age, visual health, visual acuity
		Adaptation luminance	Dark or bright adaptation
		Chromaticity	Spectral power distribution
<b>Minkowski exponent</b>	$p$	Contribution of multiple modulation frequencies (temporal waveform) and multiple spatial frequencies (luminance distribution)	

### 3.1 The contrast sensitivity function of the phantom array effect

The spatial contrast sensitivity function (CSF) characterizes the ability of an observer to discern a sinusoidal grating of a given spatial frequency. It is the inverse of the modulation depth at the visibility threshold of the modulation, expressed as a function of spatial frequency. The CSF is defined for a set of specific conditions such as: luminance of source, background and surrounding luminance, adaptation level, size and position of the stimulus, duration of the stimulus, colour features, etc. The CSF is also known to exhibit large individual differences, varying significantly with age and specific eye conditions, revealing the diversity of the population in terms of visual sensitivity.

The phantom array is visible for a very short period of time and for an observer that is not static (because of the eye saccade). Consequently, the widely used CSF models, such as the Campbell and Robson model (Campbell and Robson, 1968) are not directly applicable because they are based on data obtained with a static observer looking at a steady-state target. Therefore, the relevant CSF for the PAE still needs to be determined from experimental psychophysical data based on phantom array stimuli produced using controlled saccade speeds to accurately determine the spatial frequency of visual stimuli.

The effects of short exposure times on the CSF have been investigated by using transient gratings (Arend, 1976; Kelly 1977). With exposure durations between 10 ms and 100 ms, typical of the PAE, the contrast sensitivity is proportional to the exposure time for a given luminance level, following Bloch’s reciprocity law (Kelly, 1977). In addition, the low frequency slope of the CSF flattens when the exposure time is shortened. Shortening the exposure time reduces the low frequency decline of sensitivity relative to higher spatial frequencies at the same exposure duration.

During the eye saccade, the phenomenon of saccadic suppression causes a reduction of contrast sensitivity (Castet, 2009). Saccadic suppression is stronger for luminance stimuli with low spatial frequencies than for stimuli with high spatial frequencies (Burr et al., 1994). The magnitude of saccadic suppression decreases as spatial frequency of the gratings increases. Patterns of spatial frequencies greater than 1 cpd are not suppressed during saccades (Volkman et al, 1978).

### 3.2 An application example

An application example is given considering the CSF data reported by Volkman et al. in 1978 in their work about contrast sensitivity during a saccade (Volkman et al., 1978). The graph on the left of figure 4 shows the measured CSF data and the best fit obtained using a mathematical formula used to model the general shape of CSFs (Barten, 2003).

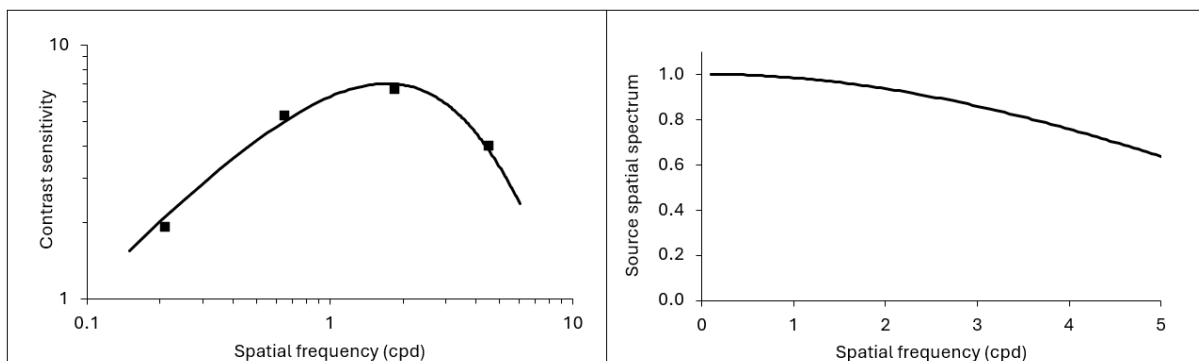


**Figure 4 – Left graph: The square dots are the CSF data reported in (Volkman et al, 1978). The line is the best fit obtained using Barten’s formula (Barten, 2003). Right graph: Spatial Fourier distribution of a 0,1° rectangular light source.**

In this example, the light source is rectangular with a width of  $l = 0,1^\circ$  and a contrast of 100 % with its surrounding. The corresponding spatial Fourier distribution is given by Equation (11):

$$\frac{\mathcal{L}(k)}{\mathcal{L}_{sur}} = \frac{\sin(\pi lk)}{\pi lk} \quad (11)$$

The graph on the right of Figure 4 shows the spatial Fourier distribution  $\mathcal{L}(k)/\mathcal{L}_{sur}$  of the light source, in the direction of the saccade.

The model can be used to determine the modulation depth of a temporal sinusoidal waveform corresponding to the visibility threshold of the PAE. In Equation (9), the visibility threshold is defined by  $V_{PA}(k) = 1$ . Therefore, the modulation depth is given by Equation (12):

$$mod(k) = \frac{\mathcal{T}(k)}{\mathcal{T}_{dc}} = \left( \frac{\mathcal{L}(k)}{\mathcal{L}_{sur}} CSF(k) \right)^{-1} \quad (12)$$

The resulting threshold modulation depth is shown in Figure 5, where the temporal modulation frequency was determined from the spatial frequency by using Equation (7) with a saccade velocity of  $400 \text{ deg}\cdot\text{s}^{-1}$ . In this example, the peak frequency of the PAE is about 640 Hz with a modulation depth of 15%. The low and high threshold frequencies are respectively 30 Hz and 2 600 Hz.

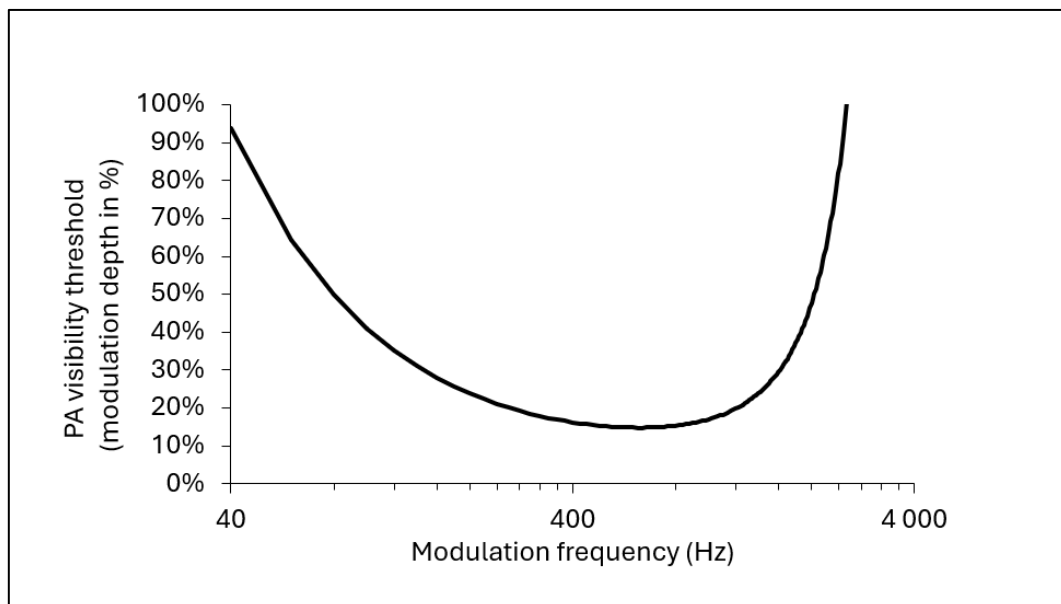


**Figure 5 – Threshold modulation depth calculated using the PAE model of Equation (9) applied using the data shown in Figure 4.**

### 3.3 The lower and upper threshold modulation frequencies and peak modulation frequency of the phantom array effect

In addition to the low and high frequency limits derived in Equations (3) and (4) from geometric considerations, the visibility model of Equation (9) implies the existence of frequency limits imposed by the behaviour of the CSF of the phantom array.

The high threshold frequency of the  $CSF_{PA}$  function is not likely to be affected by the saccadic suppression phenomenon. This threshold is about 30 cpd in photopic conditions for a standard viewer (Campbell and Robson, 1968). With typical saccade speeds between  $200 \text{ deg}\cdot\text{s}^{-1}$  and  $500 \text{ deg}\cdot\text{s}^{-1}$ , the highest modulation frequency for the phantom array would be between 6 000 Hz and 15 000 Hz, but only for light sources that are as small as  $0,05^\circ$ . Such values were experimentally reported for highly sensitive subjects looking at very thin modulated light sources (Brown et al. 2020; Kang et al. 2023b).

The low threshold frequency of the  $CSF_{PA}$  function is influenced by the saccadic suppression mechanism. The best estimate of the lowest modulation frequency of the PAE is the geometric

limit of Equation (4), defined from the requirement of having at least one phantom image between the initial and end position of the light source in the visual field.

The peak of contrast sensitivity during an eye saccade reported in (Volkman et al., 1978) is located at about 2 cpd. With typical saccade speeds of 200 deg·s<sup>-1</sup> to 500 deg·s<sup>-1</sup>, the peak modulation frequency given by Equation (7) is likely to be around 400 Hz to 1000 Hz, a range of values consistent with experimental data reported in (Kong et al., 2024; Miller et al., 2023).

### 3.4 Influence of the luminous environment and adaptation level

The luminous environment determines key aspects of the contrast sensitivity function and the resulting visibility of the PAE. The respective luminance values of the background, of the immediate surrounding, and of the light source itself, determine the adaptation state of the eye. According to the adaptation level, the CSF may have different shapes, magnitudes, and cut-off spatial frequencies (Watson et al., 1986).

The phantom array effect is a foveal phenomenon characterized by a precise image forming mechanism, where colors and contours are perfectly replicated in each phantom image. Its conspicuity at high spatial frequency can be explained by the fact that saccadic suppression preferentially acts on the information mediated by the magnocellular (M-channel) visual pathway (Burr et al., 1994) which is color-blind and carries the low frequency components from large receptive fields essentially located in the peripheral retina. For this reason, phantom arrays of intermediate and high spatial frequencies, typically above 1 cpd, are not attenuated by saccadic suppression, but reinforced by the increased contrast with the suppressed low spatial frequencies of the background.

The phantom array effect being associated with foveal vision makes it essentially a photopic phenomenon. However, its visibility depends on the luminance contrast of the modulated light source with its surrounding, making the effect much more visible in dark environments.

When moving to darker adaptation levels, the CSF decreases. The PAE being a middle and high spatial frequency phenomenon, the variation of the CSF should follow the De Vries-Rose law (Kelly, 1972), decreasing as the square root of the adaptation luminance. For instance, moving the adaptation level from 10 cd·m<sup>-2</sup> to 1 cd·m<sup>-2</sup> would lower the CSF by a factor of about 3. More comprehensive models describe how the CSF varies with the adaptation level in different ranges of temporal and spatial frequencies (Vienot et al., 2002; Watson et al., 1986). However, these models do not address the case of contrast sensitivity during an eye saccade.

### 3.5 Influence of the spectral distribution

The spectral distribution of the light source influences the visibility of the PAE, as was shown experimentally with light sources of different colours (Kang et al., 2022; Kong et al., 2023). The upper threshold frequency of the PAE is higher for green and red LEDs, in comparison to blue LEDs (Kang et al., 2022). Phantom arrays created by warm-white LEDs are also associated with higher upper threshold frequencies in comparison to cold-white LEDs. In the low frequency range, phantom arrays from red LEDs had a higher visibility than from green and warm-white LEDs (Kong et al., 2023).

In the retina, the three types of cones (S, M and L) have similar kinetics and temporal characteristics when measured at the ganglion cell level (Pietersen, 2014). Therefore, the effect of spectral distribution on the phantom array could rather be attributed to the different properties of the visual pathways involved in the phantom array. The colour and contour invariance of the phantom array suggests that it is mediated by the parvocellular (P-channel) and the koniocellular (K-channel) pathways. The P-channel exhibits red-green colour opponency, suggesting that the high frequency threshold observed with green and red LEDs should be close. The K-channel, characterized by a blue-yellow opponency, is known to be slower to process the signals of S-cones, sensitive to blue light (Pietersen, 2014), suggesting a lower high frequency threshold of the phantom array effect with blue LEDs. The lower sensitivity to the phantom array effect with blue stimuli might also be the result of S-cones being more sparsely distributed in the fovea in comparison with the M and L-cones (CIE, 2025).

## 4 Conclusions

The phantom array effect is an adverse visual effect of temporal light modulation that needs to be better understood in order to improve standards and regulations aimed at protecting both the general population and sensitive people. The studies published during the last ten years were very important to improve our understanding of this phenomenon. However, the different teams involved in studying the PAE have measured its visibility using different psychophysical protocols in different experimental conditions. Therefore, despite a fair agreement about the general behaviour of the PAE, they found different visibility curves, different threshold frequencies, different peak frequencies, and different modulation depth thresholds.

The equations we here provide are useful to predict the basic features of the PAE and to assess its visibility from simple considerations about the temporal light waveform, the luminance contrast of the light source, and the contrast sensitivity function of the observer. We use the linear theory of the human visual system to establish a general model of the PAE working in the spatial frequency domain. The model incorporates a stimulus term (spatial contrast and temporal contrast) and a response term (the contrast sensitivity function during an eye saccade). This model takes into account the combined effects of source shape, adaptation level, spatial contrast, spectral distribution, and modulation frequency.

This model is a promising framework to study the PAE considering the diversity of luminous stimuli perceived in a range of different visual conditions. The measurements of PAE visibility thresholds under well-controlled luminous conditions and saccade parameters can be used to determine the individual CSF of the PAE by inverting the model equation. This approach can be applied to existing PAE data acquired by different research teams, as well as recent data acquired during the EURAMET MetTLM project.

## Acknowledgment

This work was carried out during the MetTLM project (Metrology for Temporal Light Modulation; 20NRM01). This project ran from 2021 to 2024 with funding from the EMPIR (European Metrology Programme for Innovation and Research) programme co-financed by the Participating States and from the EU Horizon 2020 research and innovation programme.

## References

- AREND, L. (1976). Response of the human eye to spatially sinusoidal gratings at various exposure durations. *Vision Research*, 16, 1311–1315.
- BAHILL, A. T., CLARK, M. R., & STARK, L. (1975). The main sequence, a tool for studying human eye movements. *Mathematical Biosciences*, 24(3), 191–204.
- BARTEN, P. G. J. (2003). Formula for the contrast sensitivity of the human eye. In Y. Miyake & D. R. Rasmussen (Eds.), *Proc. Of SPIE Electronic Imaging 2004* (pp. 231–238).
- BROWN, E., FOULSHAM, T., LEE, C., WILKINS, A., 2020. Research Note: Visibility of temporal light artefact from flicker at 11 kHz. *Light. Res. Technol.* 52, 371–376.
- BURR, D. C., MORRONE, M. C., & ROSS, J. (1994). Selective suppression of the magnocellular visual pathway during saccadic eye movements. *Nature*, 371(6497), Article 6497
- CAMPBELL, F. W., & ROBSON, J. G. (1968). Application of Fourier analysis to the visibility of gratings. *The Journal of Physiology*, 197(3), 551–566.
- CASTET, E., & MASSON, G. S. (2000). Motion perception during saccadic eye movements. *Nature Neuroscience*, 3(2), 177–183.
- CASTET, E. (2009). Perception of Intra-saccadic Motion. In *Dynamics of Visual Motion Processing: Neuronal, Behavioral, and Computational Approaches* (pp. 213–238).
- CIE, 2022. *Visual Aspects of Time-Modulated Lighting Systems* (No. CIE 249:2022). Commission Internationale de l'Éclairage.
- CIE, 2025. *The Functional Visual Field* (No. CIE 255:2025). Commission Internationale de l'Éclairage.
- DE LANGE DZN, H., 1952. Experiments on flicker and some calculations on an electrical analogue of the foveal systems. *Physica* 18, 935–950.

- HERSHBERGER, W.A., JORDAN, J.S., 1998. The Phantom Array: A Perisaccadic Illusion of Visual Direction. *Psychol. Rec.* 48, 21–32.
- KANG, H, KIM, J., PARK, S., LEE, C.-S., PAK, H., 2022. Visibility of the phantom array effect at different LED colour temperatures under high-frequency temporal light modulation. *Light. Res. Technol.* 55 (1)
- KANG, H., LEE, C., 2023a. AN ANALYTIC APPROACH TO THE VISIBILITY MODEL OF THE PHANTOM ARRAY EFFECT, in: CIE X050:2023 Proceedings of the 30th Session of the CIE, Ljubljana, Slovenia, September 15 – 23, 2023 pp. 960–963.
- KANG, H, LEE, C.-S., KIM, J.-G., PAK, H., 2023b. Saccadic Eye Movement Speed Can Explain the Large Variations in Phantom Array Effect Visibility. *Scientific Reports* 13 (1)
- KELLY, D. H. (1972). Adaptation effects on spatio-temporal sine-wave thresholds. *Vision Research*, 12(1), 89–101.
- KELLY, D. H. (1977). Visual Contrast Sensitivity. *Optica Acta: International Journal of Optics*, 24(2), 107–129.
- KONG, X., VOGELS, R., MARTINSONS, C., TENGELIN, M., HEYNDERICKX, I., 2023. DEPENDENCE OF TEMPORAL FREQUENCY AND CHROMATICITY ON THE VISIBILITY OF THE PHANTOM ARRAY EFFECT, in: Proceedings of the 30th Quadrennial Session of the CIE “Innovative Lighting Technologies”, Ljubljana, Slovenia.
- LEE, C.-S., LEE, J.-H., PAK, H., PARK, S., SONG, D.-W., 2018. Phantom array and stroboscopic effects of a time-modulated moving light source during saccadic eye movement. *Light. Res. Technol.* 50, 772–786.
- MATIN, E. 1975. Saccadic suppression: A review and an analysis. *Psychological Bulletin*, 81, 899–917
- MARTINSONS, C., VEITCH, JENNIFER, LOUGHRAN, S., NIXON, A., MATE, R., HARRIS, R., SHEN, L., 2024. Solid-State Lighting: Review of Health Effects. International Energy Agency’s Technology Collaboration Programme on Energy Efficient End-Use Equipment (4E), Smart Sustainability in Lighting and Controls (SSLC), Stockholm, Sweden.
- MILLER, N., RODRIGUEZ-FEO BERMUDEZ, E., IRVIN, L., TAN, J., 2023. Phantom array and stroboscopic effect visibility under combinations of TLM parameters. *Light. Res. Technol.* 56 (7)
- MILLER, N.J., 2024. Correspondence: Flicker: The sneaky perception that ranges from invisible to debilitating. *Light. Res. Technol.* 56, 666–668
- PERZ, M., VOGELS, I., SEKULOVSKI, D., WANG, L., TU, Y., & HEYNDERICKX, I. (2015). Modeling the visibility of the stroboscopic effect occurring in temporally modulated light systems. *Lighting Research & Technology*, 47(3), 281–300
- PIETERSEN, A. N. J., CHEONG, S. K., SOLOMON, S. G., TAILBY, C., & MARTIN, P. R. (2014). Temporal response properties of koniocellular (blue-on and blue-off) cells in marmoset lateral geniculate nucleus. *Journal of Neurophysiology*, 112(6), 1421–1438.
- TAN, J., MILLER, N., ROYER, M., IRVIN, L., 2024. Temporal light modulation: A phantom array visibility measure. *Light. Res. Technol.* 56 (7) 772-789
- VIENOT, F., 2002. AN ALGORITHM TO ASSESS THE DETECTABILITY OF ACHROMATIC SPATIO-TEMPORAL PATTERNS AT ANY ILLUMINATION. Proceedings of the Proceedings of the CIE Symposium 2002 on "Temporal & Spatial Aspects of Light and Colour Perception and Measurement", Veszprém, Hungary
- VOLKMANN, F. C., RIGGS, L. A., WHITE, K. D., & MOORE, R. K. (1978). Contrast sensitivity during saccadic eye movements. *Vision Research*, 18(9), 1193–1199.
- WATSON, A.B., AHUMADA, A.J., FARRELL, J.E., 1986. Window of visibility: a psychophysical theory of fidelity in time-sampled visual motion displays. *JOSA A* 3, 300–307.